



# Conducting polymer coated single-walled carbon nanotube gas sensors for the detection of volatile organic compounds



Sushmee Badhulika<sup>a</sup>, Nosang V. Myung<sup>b</sup>, Ashok Mulchandani<sup>b,\*</sup>

<sup>a</sup> Department of Electrical Engineering, University of California, Riverside, CA 92521, USA

<sup>b</sup> Department of Chemical and Environmental Engineering, University of California, Riverside, CA 92521, USA

## ARTICLE INFO

### Article history:

Received 27 December 2013

Received in revised form

2 February 2014

Accepted 3 February 2014

Available online 11 February 2014

### Keywords:

Carbon nanotube

PEDOT:PSS

Electropolymerization

Gas sensor

## ABSTRACT

The current work involves fabrication, characterization and subsequent evaluation of poly(3,4-ethylenedioxythiophene) doped with poly(styrene sulfonic acid) (PEDOT:PSS) coated single walled carbon nanotubes (SWNTs) sensors for detecting analytes of interest in industrial manufacturing. By varying the conducting polymer's synthesis conditions in terms of charge controlled electropolymerization of the monomer EDOT in presence of the dopant PSS, the sensing performance of the PEDOT:PSS functionalized SWNT sensors was systematically optimized. Electrical characterization in terms of change in resistance, cyclic voltammetry and field-effect transistor measurements was performed to confirm the presence of PEDOT:PSS coating on SWNTs. The optimized sensors exhibited sensing properties over a wide dynamic range of concentrations towards saturated vapors of volatile organic compounds (VOCs) such as methanol, ethanol and methyl ethyl ketone (MEK) at room temperature. The limit of detection of this sensor was found to be 1.3%, 5.95% and 3% for saturated vapors of methanol, ethanol and methyl ethyl ketone (MEK) respectively. In terms of performance, when compared with bare SWNTs, these hybrid sensors exhibited better sensitivity. The underlying mechanism of sensing was also investigated by using them in chemFET mode of sensor configuration.

© 2014 Elsevier B.V. All rights reserved.

## 1. Introduction

Carbon nanotubes (CNTs) are being put into a variety of electronic applications such as room temperature field effect transistors [1], [2], interconnect [3] and actuators [4]. Very high electrical and thermal conductivities, extraordinary mechanical strength together with their ultrasmall size and low power consumption make them perfect candidates for being used as an electronic material [5]. Sensors constitute a field in which CNTs are being increasingly used as active material for sensing gases and vapors [6,7]. Their high surface area which consists of all surface atoms gives them the property of exhibiting high sensitivity and rapid response times towards any change in their chemical environment. The earliest attempts at using carbon nanotubes as gas sensors were made by Kong et al. in 2000 where they demonstrated bare carbon nanotubes to respond to gases like ammonia and NO<sub>2</sub> at room temperature [8]. Since then studies have shown that carbon nanotubes can be used to sense a large number of other gases and volatile organic

compounds [7,9–11]. However, gases which have low absorption capacity on carbon are difficult to be detected using single walled carbon nanotubes (SWNTs) [8]. To overcome this difficulty several techniques have been incorporated which involve modifying the surface of SWNTs using materials like conducting polymers [12,13], metals [14–17] and metal oxides [18]. Conducting polymers and their derivatives have been long used as chemical sensors. However their wide application is limited due to their inability to be used in a broad pH range [19]. Poly(3,4-ethylenedioxythiophene) doped with poly(styrene sulfonic acid) (PEDOT:PSS) is widely used in chemical sensors owing to its properties of being electrochemically active, environmentally stable and maintaining its activity over a wide pH range. The use of PSS as the counter ion renders enhanced conductivity and facilitates easier processibility [20]. Reports have been made governing the use of PEDOT nanowires and thin films towards sensing gases and alcohols [21–24].

In this work, surface functionalization of SWNTs with PEDOT:PSS using electropolymerization is reported and subsequent evaluation of the real time response of these SWNT coated PEDOT:PSS hybrid chemFET sensors towards sensing three volatile organic compounds namely methanol, ethanol and methyl ethyl ketone is performed. Electropolymerization offers a great deal of flexibility in terms of controlling the thickness of the conducting polymer film on the

\* Corresponding author. Tel.: +1 951 827 6419; fax: +1 951 827 5696.

E-mail addresses: [sbadh001@ucr.edu](mailto:sbadh001@ucr.edu) (S. Badhulika), [myung@enr.ucr.edu](mailto:myung@enr.ucr.edu) (N.V. Myung), [adani@enr.ucr.edu](mailto:adani@enr.ucr.edu) (A. Mulchandani).

surface of the SWNTs by altering parameters like charge, electrolyte composition and potential [15]. SWNTs act as the charge conduit material along with PEDOT:PSS as the sensing element which bring about an increase in the overall sensitivity of the sensors towards detection of VOCs.

## 2. Experimental

### 2.1. Sensor design and fabrication

Microfabricated gold electrodes were fabricated on highly doped p-type silicon substrate using the cleanroom facilities available at the University of California, Riverside. Briefly, a 300 nm SiO<sub>2</sub> thick film was deposited on a (100) oriented highly doped p-type Si substrate by thermal CVD deposition to insulate the substrate. It was followed by defining the drain and source electrode areas by photolithography using the positive photoresist 5214. The thickness of the chromium adhesion layer was maintained at 20 nm and that of gold above it was 180 nm. The width and gap of the electrodes were fixed at 200 μm and 3 μm, respectively.

### 2.2. SWNTs solubilization and alignment

Carboxylated-SWNTs (SWNT-COOH 80–90% purity) procured commercially from Carbon Solution, Inc., Riverside, CA, were dispersed (1 μg/mL) in dimethyl formamide obtained commercially from Sigma Aldrich, MO. Though carbon nanotubes are known to have poor solubility in most solvents, the amide group of dimethyl formamide (DMF) can attach to the surface of the nanotubes making it a suitable solvent for obtaining uniformly suspended SWNTs in DMF [8]. The suspension of SWNTs in DMF solution was prepared in steps which involved first sonicating the dispersed carboxylated SWNTs followed by centrifugation at a speed of 10,000 rpm to remove soluble fraction and aggregates.

The suspended SWNTs were aligned in the 3 μm spaced micro-fabricated gold electrodes by AC dielectrophoresis (DEP) [21]. The procedure involved addition of a 0.1 μL drop of SWNTs suspended in DMF and subsequent application of an AC voltage of 3 V peak to peak amplitude at a frequency of 4 MHz across the electrodes. The aligned SWNTs were then annealed at 300 °C for 1 h in an atmosphere of 5% hydrogen and 95% nitrogen gas to improve the contact between the electrodes and the SWNTs and to remove DMF residues accumulated during the process of SWNTs alignment.

### 2.3. Electropolymerization

Electrochemical functionalization of SWNTs with PEDOT:PSS was conducted at ambient temperature with a three electrode configuration where the aligned SWNTs network with the gold electrodes, a Pt wire, and chlorinated silver wire (Ag/AgCl wire) were used as working, counter, and reference electrodes, respectively. A 0.1 μL drop of 5 mM solution of the electrolyte EDOT (monomer) and 5 mM PSS (dopant) in water was placed on top of the SWNT networks followed by potentiostatic electropolymerization at 0.9 V vs. Ag/AgCl wire reference. The electrodes were placed in contact with the electrolyte to constitute an electrochemical cell. Charge controlled electropolymerization was performed at three different charges namely 1, 2.5 and 5 μC. After the functionalization, the sensors were washed gently with deionized water followed by blow drying lightly with nitrogen gas.

### 2.4. Device characterization and sensing

The SWNT devices were characterized before and after electropolymerization by a scanning electron microscope (SEM). SEM

images were obtained using a Zeiss Leo SUPRA 55 with beam energy of 20 kV. Sensors were characterized in terms of their current–voltage (*I*–*V*) response measured using a potentiostat (Model 1202A, CH Instruments, Inc., TX, USA) before and after electropolymerization. The voltage was swept from –1 V to +1 V and the current was recorded. The device resistance was measured as the slope of *I*–*V* near zero voltage in the linear range of ±100 mV. Transport measurements were performed using a dual channel Keithley source meter (Keithley-Model 2636A, CA) wherein the gold electrodes acted as the source and drain while polysilicon behaved as the back gate. A drain to source bias of –1 V was applied while the gate voltage was swept in the range of ±20 V at a scan rate of 0.1 V/s. Source–drain current (*I*<sub>SD</sub>) as a function of the gate voltage (*V*<sub>GS</sub>) was measured. Cyclic voltammetry was conducted in an aqueous solution of 0.1 M NaCl at a scan rate of 50 mV/s using a potentiostat (Model 1202A, CH Instruments, Inc., TX, USA).

### 2.5. Gas sensing setup

The 16 electrodes pair chip consisting of 16 individual addressable sensor devices, each electropolymerized with PEDOT:PSS were wirebonded and packaged to a 40 pin ceramic inline package, which was then mounted on to the breadboard of the sensing system setup. The sensors were connected in series with a load resistance of equal resistance value and were subject to a fixed voltage of 1 V DC. Real time measurements were carried out using a custom made sensing setup that was controlled by LabView program.

A 3.6 cm<sup>3</sup> air tight sealed glass chamber with gas inlet and outlet ports for gas flow-through was positioned over the sensor chip. Saturated vapors of the VOCs were produced by bubbling dry air through the bubbler column containing the VOC. The carrier gas in this setup was dry air. Various concentrations of the vapors were introduced to the gas chamber by regulated flow of the vapors with the help of mass flow controllers purchased from the Alicat Scientific Incorporated, Tucson, AZ. Prior to all the sensing experiments, the sensors were first exposed to dry air (purity: 99.998%) to attain a steady baseline resistance. The sensors were then exposed to different concentrations of the saturated vapors of the VOC mixed in dry air for 15 min with an interval of 20 min recovery in air between two successive vapor exposures. This constituted one complete cycle. This cycle was repeated for *n* number of times based on the range of concentrations being sensed. For real time gas sensing, the sensors thus fabricated were operated as chemiresistive sensors wherein the change in resistance upon exposure to an analyte formed the basis for measuring the sensitivity of the sensor. All sensors with an initial resistance in the range of 3–9 kΩ were used for sensing for better reliability and consistency in gas sensing results.

## 3. Results and discussions

Several techniques have been used over the past few years for fabricating carbon nanotube based semiconducting devices. They involved manipulating CNTs onto pre-patterned electrodes by an atomic force microscope [25], random dispersion of suspended carbon nanotubes onto pre-patterned electrodes, [26] and lithographically patterning catalyst [27] as CNT nucleation sites on electrode and drop casting to obtain CNT network between the electrodes. However these techniques yielded low throughput and their complexity and limited controllability rendered them unsuitable for applications which require high density sensor arrays that can be mass producible. The DEP technique eliminates such issues by offering a simple, cost-effective and controllable

alternative over such methods. In this method of alignment, the dielectrophoretic force field changes upon nanotube deposition and thereby self-limits the directed assembly to a single nanotube or nanotube bundle at pre-defined locations in the gap between the electrodes. Hence this technique offers versatility in terms of controlling the number of SWNTs bridging the electrode gap thereby making it possible to obtain nanotube based sensor devices with a desired resistance range. It is compatible with SWNTs from any source, which are suitably dispersed in an aqueous surfactant solution and can be used to align nanowires as well.

CPs can be incorporated onto the surface of CNTs either by possessing functional groups that are reactive toward CNTs [28–30] or by in situ polymerization [31]. The former approach of functionalization limits its application pool by incorporating one kind of polymer on to the surface of CNTs. In situ polymerization overcomes this issue as it enables the polymerization of a wide range of polymers on SWNTs based on doping type molecular interactions. Electropolymerization of EDOT:PSS was carried out on the surface of SWNTs to obtain a coating of the conducting polymer on the surface of SWNTs. Electropolymerization apart from being a simple, cost effective method of surface modification holds several advantages over other functionalization methods. It offers site specific electrodeposition and can be used to deposit a wide variety of nanomaterials like metals, metal oxides and semiconductors under ambient operating conditions. The thickness, grain size and the orientation of the electrodeposited material can be varied depending upon electrodeposition parameters such as electrolyte composition, deposition time and applied potential thus making it a very versatile technique of surface modification.

Structural characterization of the aligned SWNT devices was performed before and after polymerization of EDOT in an aqueous solution of the PSS on the SWNT surface. SEM images of the as fabricated SWNT device and after coating with PEDOT:PSS at optimal electropolymerization conditions are shown in Fig. 1. As can be seen, a thin film of the polymer coating is formed uniformly all over the SWNT surface. The combination of a low oxidation potential and relatively low band gap gives PEDOT its unique electrochemical and spectroscopic properties. Band gap, in case of PEDOT, is located at the transition between the visible and near-IR regions of the spectrum, thus making it strongly cathodically coloring and transmissive to visible light, sky blue transparent, in the doped and conducting state [32]. Upon electropolymerization in presence of polyelectrolyte PSS at room temperature, the change of the redox state leads to a change in the electronic structure, which was observed as an optical color transition to dark blue as confirmed from the optical microscope image (data not shown).

Additionally to confirm successful electropolymerization of PEDOT:PSS on SWNTs, electrical characterization of the coated sensors was done. These techniques involved resistance measurement; cyclic voltammetry and field-effect transistor transfer characteristics before and after electropolymerization. As can be seen in Fig. 2, the hybrid sensors exhibited a drop in resistance as compared to the bare SWNT sensors upon electropolymerization. PEDOT is a stable polymer, which exhibits relatively high electrical conductivity [33]. Furthermore, a well-processable form of this polymer is obtained by oxidative polymerization in the presence of polystyrenesulfonic acid (PSS). Charge transfer takes place between the polymer and the SWNTs upon polymerization causing an external doping that impacts the electronic structure of both the polymer and SWNTs thereby leading to a change in conductance [34,35].

As an additional confirmation of the electropolymerization, cyclic voltammograms on both bare and coated devices were performed (Fig. 3) which revealed that electropolymerization

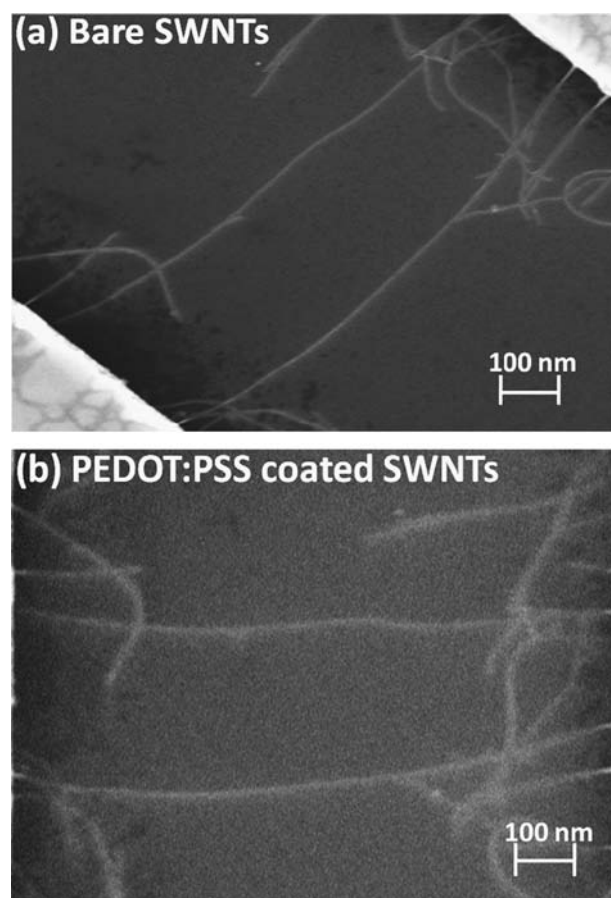


Fig. 1. SEM image of the same SWNT device before (a) and after (b) PEDOT:PSS electropolymerization.

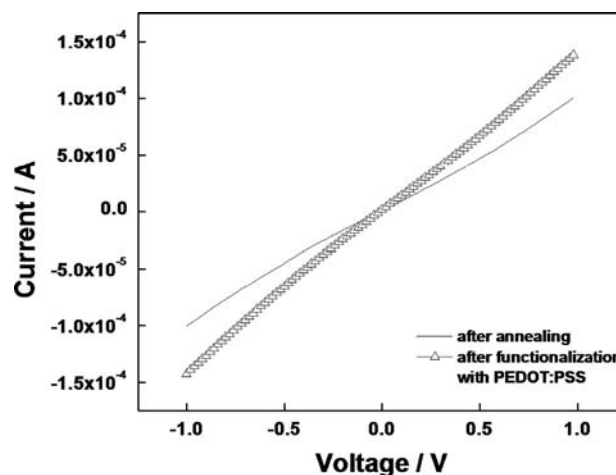


Fig. 2.  $I$ - $V$  curve of bare annealed SWNTs device before and after electropolymerization of PEDOT:PSS.

results in an increase in the current density of the PEDOT:PSS coated sensor. FET characteristics studies performed both on the bare SWNTs and the PEDOT:PSS coated SWNTs (Fig. 4) infer that the devices retain their p-type semiconducting behavior after electropolymerization with an increase in the source-drain current for all values of gate voltages applied.

Charge controlled electropolymerization was performed at several different charge conditions with an attempt to understand the effect of the electrodeposition parameter and to find a suitable charge which would result in better sensing behavior of the



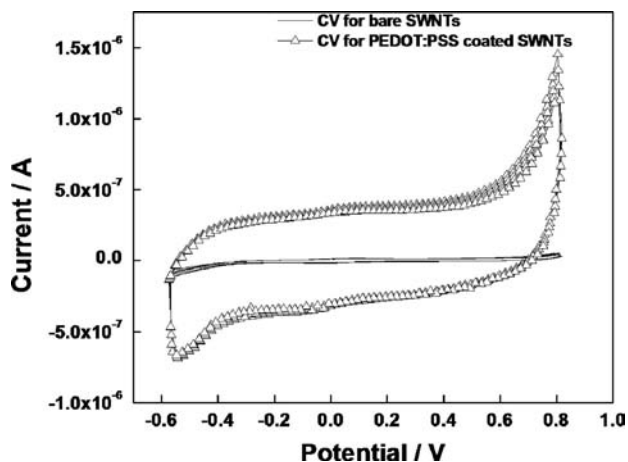


Fig. 3. Cyclic voltammograms of bare SWNTs and PEDOT:PSS coated SWNTs device; scan rate of 50 mV/s.

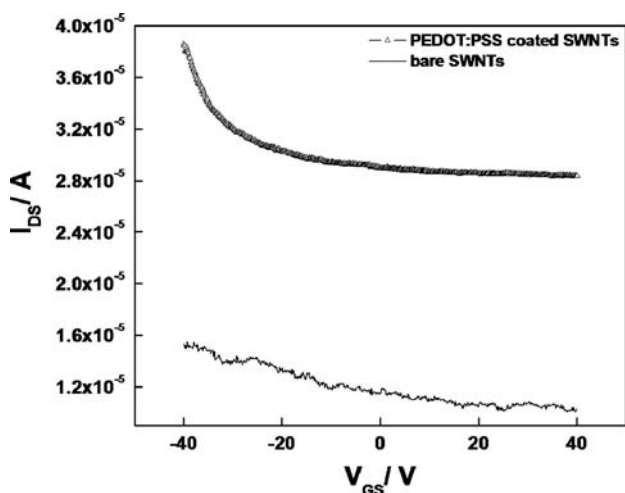


Fig. 4. Transfer characteristics curve for bare and PEDOT:PSS coated SWNTs device at  $V_{DS} = -1$  V.

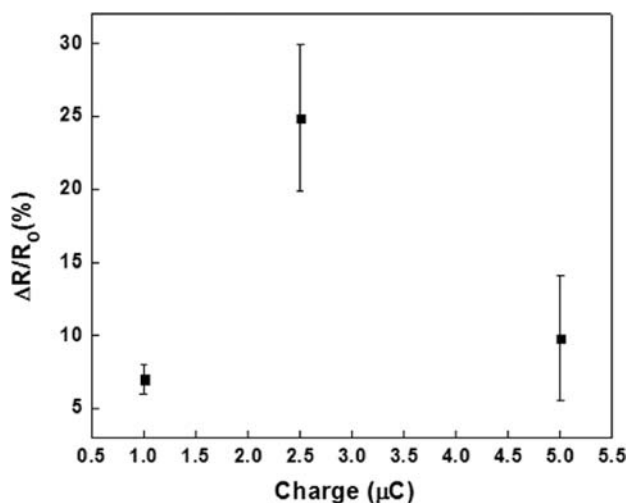


Fig. 5. Effect of PEDOT:PSS electropolymerization charge on the hybrid sensor sensitivity towards 50% saturated vapors of methanol.

PEDOT:PSS coated sensors. It was seen that for the same applied potential of 0.9 V, sensors which were coated with PEDOT:PSS at 2.5  $\mu\text{C}$  charge exhibited better dynamic sensing response than sensors coated at charges lower and higher than it (Fig. 5).

The observed trend can be attributed to the fact that at lower charge controlled electropolymerization, the PEDOT:PSS coating is too thin to enhance the performance of the sensor while at higher charges, the PEDOT:PSS coating is too thick to allow SWNTs to contribute to the sensing behavior. Hence coating the sensors at 2.5  $\mu\text{C}$  charge with PEDOT:PSS resulted in an optimum thickness of the conducting polymer that enabled a synergistic contribution of both the PEDOT:PSS coating and the SWNTs underneath to contribute to the superior performance in sensing of analytes.

Figs. 6–8 show the calibration curve along with the dynamic response of the hybrid sensor for various VOCs. The normalized response  $\Delta R/R_0$  is given by  $\{(R - R_0)/R_0\}$ , where  $R$  and  $R_0$  are the resistances in analyte gas and air, respectively. As shown in the figures, exposure to the VOCs of interest resulted in an increase in the resistance of the sensors. The hybrid sensors responded linearly to a wide range of saturated vapors of methanol i.e., from 2.5% till 75% concentrations with a limit of detection of 1.3% of saturated vapors considering a signal-to-noise ratio (SNR) of 3. While the bare SWNT devices did not respond to ethanol and MEK,

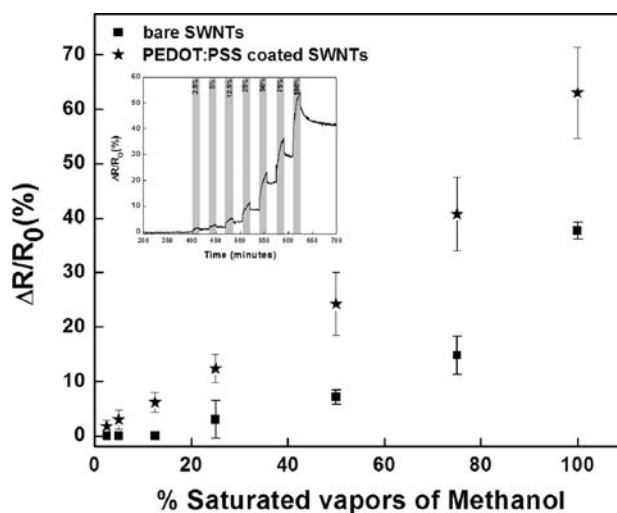


Fig. 6. Calibration curves for bare and PEDOT:PSS coated SWNTs device; dynamic response of the PEDOT:PSS coated SWNTs sensor towards different concentrations of methanol vapors (inset).

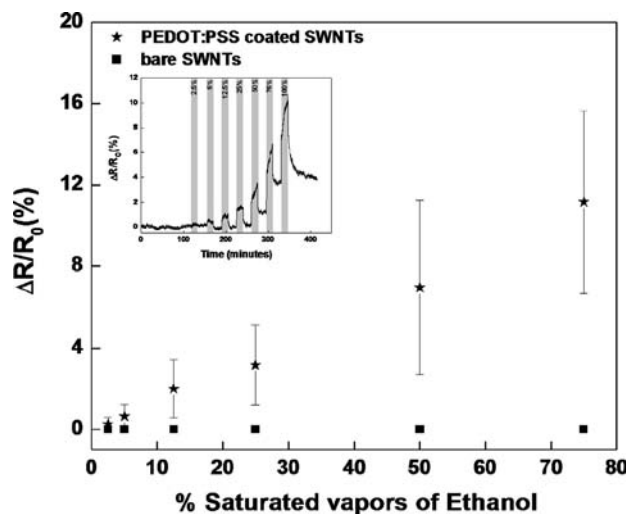


Fig. 7. Calibration curves for bare and PEDOT:PSS coated SWNTs device; dynamic response of the PEDOT:PSS coated SWNTs sensor towards different concentrations of ethanol vapors (inset).

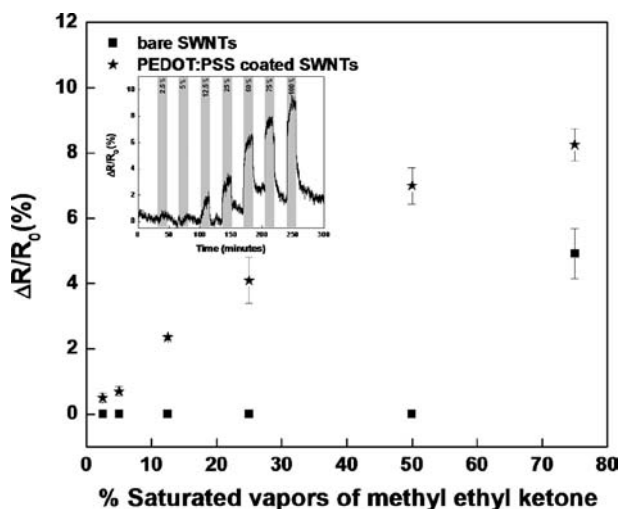


Fig. 8. Calibration curves for bare and PEDOT:PSS coated SWNTs device; dynamic response of the PEDOT:PSS coated SWNTs sensor towards different concentrations of MEK vapors (inset).

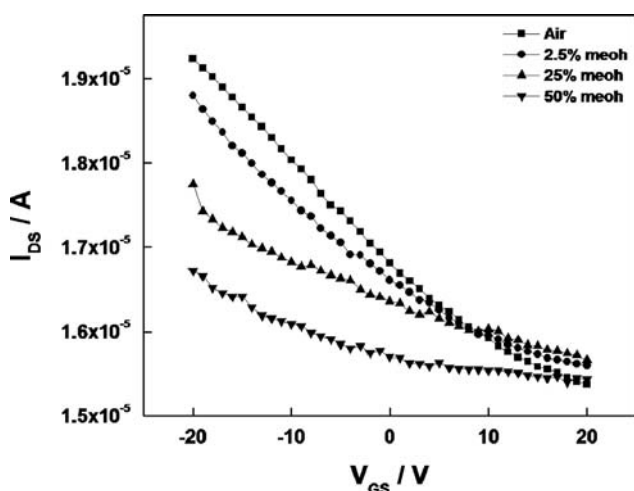


Fig. 9. Transfer characteristics curves of PEDOT:PSS coated SWNTs device when exposed to air and different saturated concentrations of methanol vapors performed at  $V_{DS} = -1$  V.

the hybrid devices responded to both the analytes. The limit of detection was calculated to be 5.95% and 3% for ethanol and MEK vapors respectively with SNR of 3.

To gain an understanding underlying mechanism governing the interaction of the PEDOT:PSS coated SWNT sensors with the analyte, the sensors were configured in the chemFET mode of operation with polysilicon as the back gate.

Fig. 9 shows the transfer characteristics i.e., current vs. gate voltage ( $I_{DS}-V_{GS}$ ) characteristics for the PEDOT:PSS coated SWNT FET device after exposure to air and then subsequent concentrations of methanol vapors at  $V_{DS}$  of  $-1$  V. Upon exposure to increasing concentrations of the analyte, there occurs a change in the slope of the transfer characteristics curve along with a shift in the threshold voltage ( $V_{TH}$ ) towards more negative voltage values of the gate voltage.  $V_{TH}$  is defined as the voltage required to deplete carriers in the channel. It can be calculated by fitting the  $I_{DS}-V_{GS}$  curve with a tangent line at the point of maximum transconductance and determining the intercept of this line with the gate voltage ( $V_{GS}$ ) axis. Methanol is an electron-donating species, and exposure to it causes a shift in the valence band away from the Fermi level, resulting in a decrease in the charge carrier (hole) concentration. This thereby causes a reduction in conductivity

and a negative shift in the threshold voltage ( $V_{TH}$ ) of the device. Thus, decrease in threshold voltage can be attributed to the electrostatic “chemical gating” of the device wherein adsorption of the analyte induces additional negative charge in the SWNT, thus n-doping the SWNT and shifting the  $I_{DS}-V_{GS}$  curve towards more negative gate voltages. In addition, there occurs a change in the mobilities (calculated from the device transconductance i.e., slope of the  $I_{DS}$  vs.  $V_{GS}$ ) of the PEDOT:PSS coated SWNT device when exposed to different saturated concentrations of methanol vapors. Thus, shift in threshold voltage along with change in mobility in the case of the device suggests that the sensing mechanism is governed both by the electrostatic gating and the Schottky barrier effects in combination [36].

A similar trend was observed also in the case of ethanol and MEK. PEDOT:PSS is soluble in water miscible solvents and in this case, high polar alcohols as well. Exposure to alcohols results in the penetration of the vapor into the organic film and in the re-dissolution of the film at high vapor concentrations. This leads to loss of conduction paths in the polymer film thereby increasing the resistance [37]. Similar explanations have also been given wherein exposure to solvent vapors results in the swelling of the polymer which in turn increases the hopping distance for charge carriers [38,39] and hence lowering of conductivity. A detailed study relating to the mechanism of interaction is required at this point.

The sensing results obtained with the PEDOT:PSS coated SWNT sensors were compared with previously reported studies based on PEDOT:PSS vapor sensors. Large area PEDOT:PSS nanowire array fabricated by using etch mask assembly of diblock copolymer was operated as an ethanol vapor sensor [40]. These high density nanowire devices exhibited a sensitivity of 1.5% for exposure to 0.5% saturated vapors of ethanol. This superior sensitivity can be attributed to the high density pattern of PEDOT:PSS nanowires between the electrodes. Ink jet printed ultrathin film PEDOT:PSS chemiresistors were also demonstrated for the detection of methanol vapors [37]. However, the irreversible change in conductivity of these PEDOT:PSS film on exposure to alcohol arising from a permanent change in its surface morphology restricts their application to one-time usage, disposable organic vapor sensors. In this current work, PEDOT:PSS coated SWNT sensors could be used to detect VOCs over a wide dynamic range of concentrations with remarkably rapid response times as compared to thick and thin film sensors [37]. Exposure to higher concentrations of saturated vapors (larger than 50%) was found to result in irreversible change in the sensor resistance. The rapid response, high sensitivity and recovery observed are consistent with the expectation of superior properties associated with the high surface-to-volume ratio, excellent transduction of these sensors and successful electrodeposition of PEDOT:PSS on the SWNT surface. Based on the current results, we expect to detect even lower concentrations of the VOCs and also be able to detect other analytes of interest.

#### 4. Conclusions

Nanogas sensors based on AC dielectrophoresis assembly of SWNT networks followed by electropolymerization of PEDOT:PSS on SWNTs surface were developed. These hybrid sensors showed response over a wide dynamic range, enhanced sensitivity over bare SWNT sensors and a lower limit of detection for saturated vapors of methanol, ethanol and MEK at room temperature. Further, incorporating different dopants and/or solvents into the PEDOT matrix can be investigated in terms of their sensing performance towards various analytes. Electropolymerization of such conducting polymers on the surface of SWNTs could endow the SWNTs with multiple tailor made materials and can become

an effective platform for the development of new kinds of nanostructured electrochemical devices with superior properties for multi-component analysis.

## Acknowledgments

We acknowledge the financial support from the Dean of the Bourns College of Engineering, University of California, Riverside.

## References

- [1] S.J. Tans, A.R.M. Verschueren, C. Dekker, *Nature* 393 (1998) 49–52.
- [2] R. Martel, T. Schmidt, H.R. Shea, T. Hertel, P. Avouris, *Appl. Phys. Lett.* 73 (1998) 2447–2449.
- [3] Z. Yao, H.W.C. Postma, L. Balents, C. Dekker, *Nature* 402 (1999) 273–276.
- [4] R.H. Baughman, C.X. Cui, A.A. Zakhidov, Z. Iqbal, J.N. Barisci, G.M. Spinks, G.G. Wallace, A. Mazzoldi, D. De Rossi, A.G. Rinzler, O. Jaschinski, S. Roth, M. Kertesz, *Science* 284 (1999) 1340–1344.
- [5] J.S. Hwang, H.T. Kim, H.K. Kim, M.H. Son, S.W. Hwang, D. Ahn, *Phys. Status Solidi B – Basic Solid State Phys.* 246 (2009) 744–746.
- [6] D.R. Kauffman, A. Star, *Angew. Chem. Int. Ed.* 47 (2008) 6550–6570.
- [7] J. Li, Y.J. Lu, Q. Ye, M. Cinke, J. Han, M. Meyyappan, *Nano Lett.* 3 (2003) 929–933.
- [8] J. Kong, N.R. Franklin, C.W. Zhou, M.G. Chapline, S. Peng, K.J. Cho, H.J. Dai, *Science* 287 (2000) 622–625.
- [9] H.Q. Nguyen, G.Y. Cha, J.B. Yu, J.S. Huh, *Rare Met. Mater. Eng.* 35 (2006) 188–189.
- [10] H.Q. Nguyen, J.S. Huh, *Sens. Actuators B – Chem.* 117 (2006) 426–430.
- [11] T. Ueda, M.M.H. Bhulyan, H. Norimatsu, S. Katsuki, T. Ikegami, F. Mitsugi, *Phys. E – Low-Dimens. Syst. Nanostruct.* 40 (2008) 2272–2277.
- [12] S. Srivastava, S.S. Sharma, S. Kumar, S. Agrawal, M. Singh, Y.K. Vijay, *Int. J. Hydrog. Energy* 34 (2009) 8444–8450.
- [13] D.N. Huyen, N.D. Chien, *J. Korean Phys. Soc.* 52 (2008) 1364–1367.
- [14] A. Star, V. Joshi, S. Skarupo, D. Thomas, J.C.P. Gabriel, *J. Phys. Chem. B* 110 (2006) 21014–21020.
- [15] S. Mubeen, T. Zhang, B. Yoo, M.A. Deshusses, N.V. Myung, *J. Phys. Chem. C* 111 (2007) 6321–6327.
- [16] D.R. Kauffman, D.C. Sorescu, D.P. Schofield, B.L. Allen, K.D. Jordan, A. Star, *Nano Lett.* 10 (2010) 958–963.
- [17] S. Mubeen, T. Zhang, N. Chartuprayoon, Y. Rheem, A. Mulchandani, N.V. Myung, M.A. Deshusses, *Anal. Chem.* 82 (2010) 250–257.
- [18] W. Wongwiriyan, S. Inoue, Y. Okabayashi, T. Ito, R. Shimazaki, T. Maekawa, K. Suzuki, H. Ishikawa, S. Honda, H. Mori, K. Oura, M. Katayama, *Appl. Phys. Express* 2 (2009) 095008–095011.
- [19] M. Nikolou, G.G. Malliaras, *Chem. Rec.* 8 (2008) 13–22.
- [20] F. Jonas, W. Krafft, B. Muys, *Macromol. Symp.* 100 (1995) 169–173.
- [21] Y.P. Dan, Y.Y. Cao, T.E. Mallouk, A.T. Johnson, S. Evoy, *Sens. Actuators B – Chem.* 125 (2007) 55–59.
- [22] Y.P. Dan, Y.Y. Cao, T.E. Mallouk, S. Evoy, A.T.C. Johnson, *Nanotechnology* 20 (2009) 434014–434018.
- [23] C.Y. Lin, J.G. Chen, C.W. Hu, J.J. Tunney, K.C. Ho, *Sens. Actuators B – Chem.* 140 (2009) 402–406.
- [24] C.M. Hangarter, S.C. Hernandez, X.I. He, N. Chartuprayoon, Y.H. Choa, N.V. Myung, *Analyst* 136 (2011) 2350–2358.
- [25] L. Roschier, R. Tarkkiainen, M. Ahlskog, M. Paalanen, P. Hakonen, *Microelectron. Eng.* 61–2 (2002) 687–691.
- [26] A. Bezryadin, A.R.M. Verschueren, S.J. Tans, C. Dekker, *Phys. Rev. Lett.* 80 (1998) 4036–4039.
- [27] N.R. Franklin, Q. Wang, T.W. Tomblor, A. Javey, M. Shim, H.J. Dai, *Appl. Phys. Lett.* 81 (2002) 913–915.
- [28] Y.Q. Liu, Z.L. Yao, A. Adronov, *Macromolecules* 38 (2005) 1172–1179.
- [29] Y.L. Liu, W.H. Chen, *Macromolecules* 40 (2007) 8881–8886.
- [30] Y.L. Liu, Y.H. Chang, M. Liang, *Polymer* 49 (2008) 5405–5409.
- [31] K.P. Lee, A.M. Showkat, A.I. Gopalan, S.H. Kim, S.H. Choi, S.H. Sohn, *J. Appl. Polym. Sci.* 101 (2006) 3721–3729.
- [32] L. Groenendaal, F. Jonas, D. Freitag, H. Pielartzik, J.R. Reynolds, *Adv. Mater.* 12 (2000) 481–494.
- [33] Q.B. Pei, G. Zuccarello, M. Ahlskog, O. Inganas, *Polymer* 35 (1994) 1347–1351.
- [34] M. Kalbac, L. Kavan, L. Dunsch, *Synth. Met.* 159 (2009) 2245–2248.
- [35] M. Kalbac, L. Kavan, M. Zukalova, L. Dunsch, *Carbon* 45 (2007) 1463–1470.
- [36] I. Heller, A.M. Janssens, J. Mannik, E.D. Minot, S.G. Lemay, C. Dekker, *Nano Lett.* 8 (2008) 591–595.
- [37] M.F. Mabrook, C. Pearson, M.C. Petty, *Appl. Phys. Lett.* 86 (2005) 013507–013510.
- [38] Y. Cao, A.E. Kovalev, R. Xiao, J. Kim, T.S. Mayer, T.E. Mallouk, *Nano Lett.* 8 (2008) 4653–4658.
- [39] H. Bai, G.Q. Shi, *Sensors* 7 (2007) 267–307.
- [40] C.A. Ross, Y.S. Jung, W. Jung, H.L. Tuller, *Nano Lett.* 8 (2008) 3776–3780.